



Smart Sensor Technologies for Ultra-Sensitive Hydrogen Peroxide Detection in Biomedical Applications

Dr. K. Saritha Rani,

Assistant Professor of Chemistry, MVS Govt. Arts & Science College(A), Mahabubnagar

Email Id: ksrsaritharani@gmail.com

Abstract

Hydrogen peroxide (H_2O_2) is a key molecule involved in various physiological and pathological processes and is widely used as a biomarker in biomedical diagnostics. However, the detection of low concentrations of H_2O_2 , particularly those released by cancer cells, remains a significant challenge for existing sensing technologies. This study presents a comprehensive overview of three innovative approaches to address this limitation through the integration of nanotechnology, microfluidics, and machine learning. First, a plasmonic-enhanced nanopatterned microfluidic platform coupled with an Amplex Red assay demonstrated a detection limit of 1 pM and improved reaction kinetics by approximately sevenfold. Image-based analysis using a machine learning algorithm achieved 91% accuracy in classifying H_2O_2 concentrations in breast and prostate cancer media. Second, a portable, non-enzymatic microfluidic paper-based analytical device (μPAD) using a TMB–KI colorimetric system was developed alongside a smartphone application, *Hi-perox Sens*, enabling robust detection under varied lighting conditions with a classification accuracy of 97.8%.

Finally, machine learning was applied to optimize the synthesis of carbon quantum dots (CDs), enhancing quantum yield by up to 200% and enabling fluorescence-based detection of H_2O_2 in human teeth with a detection limit of 0.12 M. Collectively, these approaches highlight the potential of combining smart materials and machine learning for the development of sensitive, adaptable, and user-friendly H_2O_2 detection systems suitable for clinical and environmental applications.

Key words: H_2O_2 detection, machine learning, microfluidics, μPAD , quantum dots

1. Introduction

Hydrogen peroxide (H_2O_2) plays key roles in biological systems as a regulator and signaling molecule, especially in cancer-related cell growth.^[1-3] However, its low cellular concentrations make detection challenging for current methods.^[4] While several techniques exist—including electrochemistry,^[5]

fluorescence,^[6] and colorimetry^[7]—colorimetric assays stand out for their simplicity, low cost, and potential for portable use. The Amplex Red assay, which produces a visible pink color when detecting H_2O_2 , is commonly used in labs and has shown promise when combined with nanostructures.^[8] Still, improving sensitivity is essential for adapting such assays to point-of-care applications.

Plasmonic materials can enhance colorimetric assays by boosting color intensity through light-driven processes. When illuminated, plasmonic nanostructures like nanodisks or nanorods generate hot carriers that can trigger photocatalytic reactions, improving assay sensitivity.^[9] These structures, made from metals like gold,^[10] silver,^[11] or aluminum,^[12] are tunable by altering their shape and size. Traditional fabrication methods like e-beam lithography are costly and complex, but alternatives like colloidal lithography offer scalable, simpler nanopatterning.^[13-15]

To create a more portable and user-friendly system, plasmonic substrates are integrated into a microfluidic device. This chip features three parallel channels fed by a single inlet and allows easy sample loading using syringe pumps. It enables precise control, low reagent use, and rapid, high-throughput testing. For better analysis, the colorimetric results are captured, digitized, and analyzed using machine learning to classify H_2O_2 levels accurately.

In this review, one-step multiplexed device featuring a nanostructured plasmonic platform that enables highly sensitive colorimetric detection of H_2O_2 , a key marker of cancer cell metabolism is discussed.^[16] The device integrates a machine learning-based Random Forest classifier to analyze color changes and classify samples as either “high” or “low-to-no” H_2O_2 concentration (Figure 1).^[16] This work highlights the potential of translating lab-based colorimetric assays into compact, automated tools for detecting H_2O_2 in physiological and cancer-related processes.

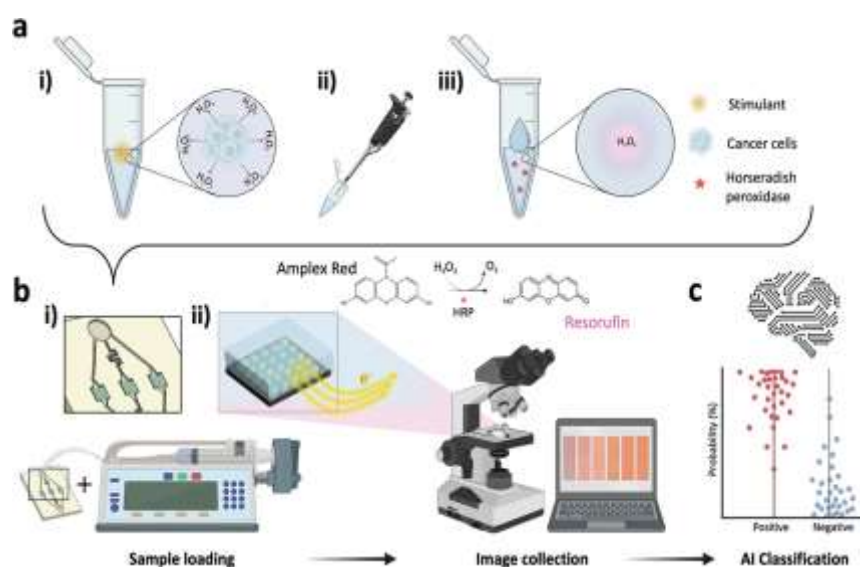


Figure 1 ^[16]

a) The cancer cell screening assay starts with i) a tube/plate with the cancer cells and a stimulant, Phorbol-12-myristate-13-acetate (PMA), is added to promote the cell's release of H_2O_2 to the media. ii) The cell media is collected and iii) combined with the assay's working solution containing Amplex Red reagent and horseradish peroxidase (HRP). b) When the mix is introduced into the microfluidic device it is delivered to i) the three detection chambers where the readout is ii)

enhanced by the nanostructured platform during the imaging through a brightfield microscope. c) The data collected is then fed to an AI classifier for the sample state determination. Figure created with Biorender.

2. Literature Review

Hydrogen peroxide (H_2O_2), a reactive oxygen species, plays a crucial role in cellular signaling and regulation, particularly in cancer cell metabolism. Elevated levels of intracellular H_2O_2 are often linked to oxidative stress and tumor progression, making it a promising biomarker for early cancer detection. Several techniques have been developed for H_2O_2 detection, including:

Electrochemical sensors: Offer high sensitivity but often require complex fabrication and are not ideal for portable use.^[5]

Fluorescence-based assays: Provide good sensitivity and specificity but are costly and need sophisticated equipment.^[6]

Colorimetric assays (e.g., Amplex Red): Widely used due to their simplicity, cost-effectiveness, and visual readability, but they typically lack the sensitivity needed for detecting low H_2O_2 levels in biological samples.^[7]

Plasmonic nanostructures have been explored to enhance assay sensitivity by amplifying the colorimetric response through light-matter interactions.^[16]

Recently, integration with **microfluidic platforms** and **machine learning** has shown potential to enhance precision, enable automation, and reduce human error in diagnostics.

In the present review paper the second sensor based technique for detection of H_2O_2 is: iodide-mediated 3,3',5,5'-tetramethylbenzidine (TMB)- H_2O_2 reaction system applied to a microfluidic paper-based analytical device (μPAD) for non-enzymatic colorimetric determination of H_2O_2 .^[17] The proposed system is portable and incorporates a μPAD with a machine learning-based smartphone app. A smartphone app called “*Hyperox Sens*” capable of image capture, cropping and processing was developed to make the system simple and user-friendly.^[17]

The third sensor based technique for detection of H_2O_2 is by using Carbon quantum Dots (CDs). CDs are applied as fluorescent probes to monitor hydrogen peroxide (H_2O_2) in human teeth.^[18]

Not only the techniques which are discussed above, a lot of articles have been published regarding the detection of (H_2O_2), such as sulphur-doped graphene (SG) is used for making highly sensitive and selective electrochemical sensor platform for accurate quantification of Hydrogen Peroxide (H_2O_2).^[19]

There is a critical need for developing cost-effective, portable, and highly sensitive detection systems for H_2O_2 in cancer cells. Systems that integrate plasmonic enhancement, microfluidic platforms, and machine

learning-based analysis represent a promising direction to fill this gap and enable practical diagnostic applications.

3. Significance of the Study

This study addresses the limitations of current H₂O₂ detection methods by developing a low-cost, multiplexed microfluidic device integrated with plasmonic nanostructures and a machine learning-based classification system. The platform enhances colorimetric detection sensitivity, enables automated readout analysis, and allows for easy operation in clinical or field settings. By providing a reliable and accessible method to detect H₂O₂—a key indicator of cancer cell activity—this article contributes to advancing early cancer diagnostics, improving disease monitoring, and promoting the development of portable, point-of-care biosensing technologies.

4. Materials and Methods

4.1 Cell Culture and Preparation

Five human cell lines were selected for this study to simulate both oncogenic and physiological conditions. Cancerous lines included MCF-7 (human breast adenocarcinoma) and PC3 (prostate adenocarcinoma), while non-cancerous controls consisted of hVFF (human vocal fold fibroblasts), HDF (human dermal fibroblasts), and CBFE (human corneal basal epithelial cells). All cell lines were cultured in their respective complete growth media under standard incubation conditions (37 °C, 5% CO₂) and harvested at ~80% confluency. Cell concentrations were standardized to approximately 1×10^6 cells/mL for experimental consistency.

4.2 Hydrogen Peroxide Stimulation

To induce reactive oxygen species (ROS) production, cells were treated with phorbol-12-myristate-13-acetate (PMA) at concentrations ranging from 0 to 200 nM for 30 minutes prior to testing. PMA acts via protein kinase C activation to stimulate oxidative burst and intracellular H₂O₂ release. Following incubation, cells were washed and suspended in phosphate-buffered saline (PBS) or PBS-diluted plasma (10%) to mimic physiological conditions. Control groups were treated identically but received no PMA.

4.3 Plasmonic Substrate Fabrication

Plasmonic substrates were prepared using a modified colloidal lithography technique. Polystyrene (PS) microspheres (500 nm diameter) were self-assembled into a close-packed hexagonal monolayer on silicon wafers. A thin plasmonic film (~30–50 nm of Au or Al) was deposited via thermal evaporation. This configuration enabled localized surface plasmon resonance (LSPR) enhancement and amplified optical responses during colorimetric detection.

4.4 Microfluidic Device Design and Integration

Microfluidic devices were fabricated via soft lithography using polydimethylsiloxane (PDMS). Each chip comprised one sample inlet, three parallel microchannels for multiplexed detection, and reaction chambers aligned with the plasmonic substrates. PDMS layers were plasma-bonded to glass or silicon wafers containing the nanopatterned metal surface. The device was syringe-actuated, requiring only a single step for sample loading and distribution.

4.5 Colorimetric Detection Assay

Hydrogen peroxide detection was achieved via the Amplex Red assay. Amplex Red (10-acetyl-3,7-dihydroxyphenoxazine) reacts with H_2O_2 in the presence of horseradish peroxidase (HRP) to form resorufin, a fluorescent red dye detectable by eye and imaging. The assay mixture (Amplex Red + HRP) was pre-mixed with the cell suspension and loaded into the device. Following a 15-minute reaction period, images of the detection chambers were captured using a high-resolution CMOS imaging setup under standardized illumination.

4.6 Image Processing and Statistical Analysis

Captured images were processed using Python libraries (OpenCV, NumPy) to extract colorimetric features (RGB and HSV values). Color matrices were generated and normalized across all triplicate samples. One-way ANOVA with Tukey's post hoc test was used to assess statistical significance in color intensity among cell types. Variability in morphology and metabolic rates between cell lines was acknowledged and accounted for in quantitative comparisons.

4.7 Machine Learning Classification

Colorimetric data were converted into numerical vectors for supervised machine learning. The dataset was split into training (70%) and test (30%) sets. A random forest (RF) classifier and a support vector machine (SVM) with an RBF kernel were trained to categorize samples as "high H_2O_2 concentration" (positive) or "low-to-no H_2O_2 concentration" (negative).^[20-22] Model performance was evaluated using accuracy metrics, confusion matrices, and receiver operating characteristic (ROC) curves. The RF model yielded superior classification performance, achieving an accuracy of 91% and an AUC of 0.96.

5. Results and Discussion Analysis

5.1 H_2O_2 Colorimetric Signal Generation

The study begins by describing the integration of a nanopatterned plasmonic platform for enhanced H_2O_2 colorimetric detection. The key component is a colorless Amplex Red solution, which reacts with H_2O_2 in a one-step assay. This solution contains the Amplex Red reagent and horseradish peroxidase (HRP) enzyme.

The enzyme catalyzes the oxidation of Amplex Red into resorufin, a fluorescent pink dye, signaling the presence of H_2O_2 . The study confirms that the assay performs specifically for H_2O_2 .^[23-24]

To enhance the sensitivity of this colorimetric assay, the nanopatterned plasmonic platform is utilized. The platform leverages localized surface plasmon resonance (LSPR), which amplifies the signal due to enhanced light-matter interactions at the nanoparticle surfaces. By adjusting the physical parameters of the platform, the color gamut of the assay is broadened, allowing for better monitoring of the solution's color change. The Al platform (aluminum) with a 400 nm diameter bead pattern demonstrated the largest color change in response to varying H_2O_2 concentrations, making it the most promising material for integration into the fluidic device. The FE-SEM and AFM analyses confirmed that the platform's morphology was consistent, and the quality of the nanopattern is critical for reproducible results. These characterizations emphasize the importance of nanopattern design in enhancing the colorimetric response, which depends on LSPR effects driven by nanoparticle geometry. (Figure 2)^[16]

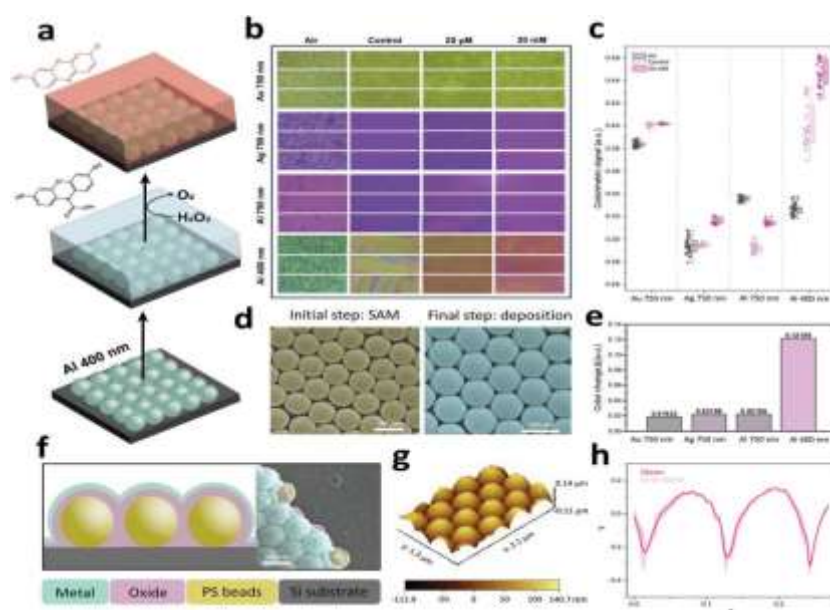


(Figure 2)

Color signal generation and characterization of the nanostructured platform. a) Schematic of the assisting nanopatterned plasmonic platform, platform in working solution, and the solution color change in the presence of H_2O_2 . b) Performance assessment of the assisting nanopatterned plasmonic platform. The color rendered by different platforms with various particle diameters and material combinations (y-axis) over the presence of different media conditions (x-axis). c) The colorimetric signal readout of the color palette in b) confirms the wider gamut of the Al 400 nm platform compared to the others. d) The fabless self-assembly monolayer (SAM) before and after the thin plasmonic layer deposition. The difference in the plasmonic generated color of the various platforms tested renders a different initial point for the color change, e) the color change delta is plotted considering the colorimetric signal in air and at 20 mM conditions. The platform with the highest delta is the selected one to move forward with the rest of the study. f) The cross-section of the platform, cartoon, and SEM, allows us to see the different layers that integrate it, from bottom to top: Si substrate, PS beads SAM, oxide layer, and a plasmonic metal layer. g) The platform was also characterized via AFM, and a 3D model and a h) roughness profile demonstrate the uniformity of deposition and of the pattern created by the PS-bead monolayer.

5.2 Nanostructured Platform Optimization

The plasmonic properties of the nanopatterned platform are highly dependent on nanoparticle size and shape, as these factors determine the LSPR effect, a phenomenon that enhances local electromagnetic fields. The platform's optimization was carried out using finite-difference time-domain (FDTD) simulations to study the electric field distribution around nanoparticles of varying sizes (200, 400, 600, and 750 nm). The 400 nm diameter bead showed the highest electromagnetic field enhancement and, as expected, produced the most

effective plasmonic response. This finding was corroborated by experimental data, where the 400 nm Al beads provided the highest enhancement in both field distribution and reflectance spectra (Figure 3). The gaps between adjacent beads further amplified the local electromagnetic field, contributing to better interaction with the H₂O₂ during the assay.

The platform's simulation results highlight the importance of bead size in optimizing the plasmonic response and enabling the enhanced detection of H₂O₂. The ability to adjust bead diameter to maximize the EM-field distribution directly influenced the platform's sensitivity to H₂O₂.

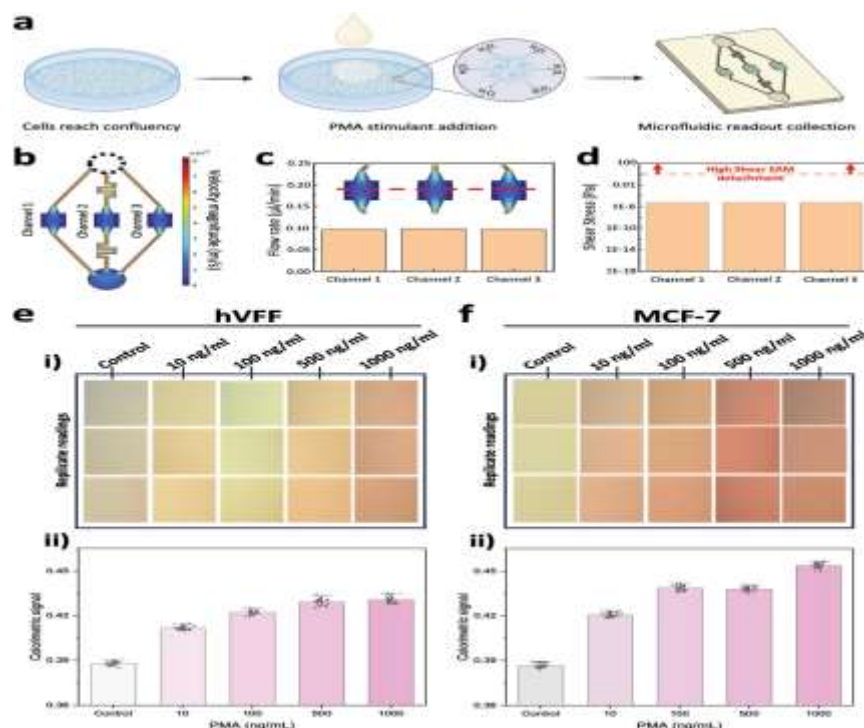
5.3 H₂O₂ Colorimetric Detection Sensitivity

The selected 400 nm Al nanopatterned platform was tested for its ability to enhance the colorimetric detection of H₂O₂ using the Amplex Red assay. The presence of H₂O₂ resulted in a color change from pale green to orange, correlating with increasing concentrations of H₂O₂ in PBS samples. The limit of detection (LOD) was determined to be as low as 1 pM, which is lower than many previously reported colorimetric assays for H₂O₂ detection (Table S1, Supporting Information). The linear correlation ($R^2 = 0.98$) between H₂O₂ concentration and the colorimetric signal further validates the platform's high sensitivity and its potential for real-world applications, where extremely low concentrations of biomarkers are often crucial for early diagnosis.

5.4 One-Step Multiplexed Microfluidic Device

The study also addresses the need to streamline the colorimetric assay process, particularly the critical step of mixing cell culture media with the Amplex Red reagent. To eliminate human variability and improve reproducibility, a multiplexed microfluidic chip was designed. This chip allows for precise control over sample delivery, ensuring consistent and reproducible results in multiple independent channels. The 3D-printed microfluidic chip is connected to a syringe pump that controls the movement of the sample fluid, and the device was computationally validated for equal hydraulic resistance across its channels. The fluid dynamics were carefully designed to avoid any detachment of the nanopatterned plasmonic substrate due to shear stress from fluid flow. This integration into a microfluidic device is essential for automating the process and facilitating high-throughput analysis.

(Figure 3) [16]



Multiplexed microfluidic device for Amplex red colorimetric assay detection of H₂O₂ in cells model. a) The cell lines are cultured until 80% confluency and the stimulant is added, which increases the release of the H₂O₂ from the cell to the media. The media is collected and mixed with the color detection assay, next it is loaded into the fluidic device and delivered to the detection chamber for image collection in triplicates. COMSOL Multiphysics simulation of d) hydraulic resistance simulation of the flow rate present in the three channels where c) the flow rate was found to be at the start point of the detection chamber. d) the shear stress experienced in the three channels. Once the device was characterized, The device is loaded with the color assay solution to test e) non-cancerous and f) cancerous cell lines. e-i) and f-i) Color matrixes represent three example areas of the detected colorimetric readout of the cell lines being exposed to four concentrations of PMA (10, 100, 500, and 1000 ng mL⁻¹). e-ii) and f-ii) Magnitude of the colorimetric signal for each of the conditions tested (N = 30).

Discussion and Insights

1.Nanopatterned Plasmonic Platform: The Aluminum (Al) platform, with a 400 nm bead size, provided the largest color change and the best enhancement of the LSPR effect for colorimetric detection. This result suggests that platform optimization (in terms of nanoparticle size and material) is crucial for increasing sensitivity.

The careful morphological analysis using FE-SEM and AFM helped ensure consistent platform fabrication, which is key for reproducible results.

2.Sensitivity and Detection Limits: The integration of the nanopatterned plasmonic platform with the Amplex Red assay significantly improved sensitivity, enabling detection of H₂O₂ at concentrations as low as 1 pM, which is an improvement over conventional methods. This high sensitivity positions the platform as a strong candidate for early cancer detection, where low-level biomarker detection is critical.

3.Microfluidic Integration: The development of a multiplexed microfluidic chip addresses one of the challenges of colorimetric assays: human error in mixing and transferring the sample. With automated sample delivery and controlled fluid movement, the system ensures uniform conditions across multiple assays, further improving reproducibility.

4. Finite-Difference Time-Domain (FDTD) Simulations: Simulations were conducted to investigate the optical properties of nanopatterned plasmonic structures. A plane-wave excitation with wavelengths spanning the visible spectrum (380–720 nm) was used. Particle sizes of 200, 400, 600, and 750 nm were modeled, with special focus on 400 and 750 nm sizes. The FDTD simulations were performed using the Lumerical FDTD Solutions software (v8.21.1781, Lumerical Solutions, Inc.) to study plasmonic resonances and light-matter interactions.

5. Electrochemical Measurements: Electrochemical experiments were conducted using an Autolab PGSTAT204 potentiostat/galvanostat with a conventional three-electrode setup. A nanopatterned plasmonic platform was used as the working electrode, with Ag/AgCl and platinum wire serving as the reference and counter electrodes, respectively.

Electrochemical Impedance Spectroscopy (EIS): Measurements were performed using H₂O₂ as a probe.

Chronoamperometric Testing: Conducted to assess the photoresponse under ambient light conditions at a bias potential of 1 V versus the reference electrode, with varying concentrations of Amplex Red reagent. All experiments were performed in PBS.

In iodide-mediated 3,3',5,5'-tetramethylbenzidine (TMB)-H₂O₂ reaction system applied to a microfluidic paper-based analytical device (μ PAD) for non-enzymatic colorimetric determination of H₂O₂, Circular μ PADs were developed and evaluated using varying concentrations of H₂O₂. After the colorimetric reaction, images of the μ PADs were captured using four different smartphones under seven distinct lighting conditions. To enhance the system's robustness against variations in illumination and camera characteristics, image data were processed for feature extraction and subsequently used to train machine learning classifiers. Among the tested conditions, the combination of TMB and KI achieved the highest classification accuracy of 97.8%, demonstrating consistent inter-phone repeatability at $t = 30$ s across diverse lighting environments, with stable performance maintained for up to 10 minutes. Furthermore, the system's performance in real samples was comparable to that of two commercially available H₂O₂ test kits.

In the detection of H₂O₂ by using Carbon quantum Dots (CDs). CDs are applied as fluorescent probes to monitor hydrogen peroxide (H₂O₂) in human teeth.^[18] The CD probe demonstrates a linear response to H₂O₂ concentrations ranging from 0 to 1.1 M, with a detection limit as low as 0.12 M, making it effective for detecting residual H₂O₂ following tooth bleaching procedures. This study highlights the significant advantages of applying machine learning techniques to guide the synthesis of high-quality carbon dots (CDs), potentially accelerating the development of other advanced functional materials for applications in energy, biomedicine, and environmental remediation.

6. Challenges and Considerations

Variability in Cell Types: The differences in H₂O₂ production across cell types (MCF-7 vs. PC3) highlight the complexity of biological systems. Despite statistical significance, the variation in H₂O₂ levels between cancerous cell lines may suggest that the platform's performance may be influenced by other factors such as cell morphology, metabolism, and extracellular matrix interactions.

Quantitative Analysis Challenges: While qualitative detection (positive vs. negative) works well, obtaining highly quantitative H₂O₂ measurements may be challenging due to the inherent variability in cellular behaviors and H₂O₂ release. These challenges should be addressed in future work by refining the platform and exploring other techniques for more precise quantification.

Optimization for Clinical Use: The translation of this system into clinical applications will require further validation in clinical samples (i.e., patient-derived cells or tissues). Additionally, robustness and consistency of the platform need to be established, especially in complex biological environments like plasma, which was used in this study as a simulated physiological condition.

7. Conclusion and Future Directions

The study successfully demonstrates the ability of a nanopatterned plasmonic platform coupled with machine learning to detect elevated H₂O₂ levels in cancerous cells. This work contributes to the growing field of biosensors for cancer detection and highlights the potential of colorimetric assays in automated, portable diagnostic devices. Future work may involve optimizing the platform for clinical use, enhancing its quantitative capabilities, and testing it in clinical settings to further establish its utility in cancer diagnostics.

8. References

1. Bai, W., Zhang, X., Zhang, S., Sheng, Q., & Zheng, J. (2017). Acidification of manganese dioxide for ultrasensitive electrochemical sensing of hydrogen peroxide in living cells. *Sensors and Actuators B: Chemical*, 242, 718–727. <https://doi.org/10.1016/j.snb.2016.11.125>
2. Zhang, Y., Bai, X., Wang, X., Shiu, K.-K., Zhu, Y., & Jiang, H. (2014). Highly sensitive graphene–Pt nanocomposites amperometric biosensor and its application in living cell H₂O₂ detection. *Analytical Chemistry*, 86(19), 9459–9465. <https://doi.org/10.1021/ac5009699>
3. Li, L., Zhang, Y., Zhang, L., Ge, S., Liu, H., Ren, N., ... & Yu, J. (2016). based device for colorimetric and photoelectrochemical quantification of the flux of H₂O₂ releasing from MCF-7 cancer cells. *Analytical Chemistry*, 88(10), 5369–5377.
4. Trachootham, D., Alexandre, J., & Huang, P. (2009). Targeting cancer cells by ROS-mediated mechanisms: a radical therapeutic approach?. *Nature reviews Drug discovery*, 8(7), 579–591.
5. del Real Mata, C., Moakhar, R. S., Hosseini, I. I., Jalali, M., & Mahshid, S. (2021). A nanostructured microfluidic device for plasmon-assisted electrochemical detection of hydrogen peroxide released from cancer cells. *Nanoscale*, 13(34), 14316–14329.
6. Sun, H., Xu, Q., Ren, M., & Kong, F. (2024). A biocompatible chitosan-based fluorescent polymer for efficient H₂O₂ detection in living cells and water samples. *International Journal of Biological Macromolecules*, 257, 128760.
7. Ma, S., Wei, C., Bao, Y., Liu, Y., Jiang, H., Tong, W., ... & Huang, X. (2024). Modular coupling MOF nanozyme with natural enzyme on hollow fiber membrane for rapid and reusable detection of H₂O₂ and glucose. *Microchimica Acta*, 191(2), 107.
8. Singh, S., Cortes, G., Kumar, U., Sakthivel, T. S., Niemiec, S. M., Louiselle, A. E., ... & Seal, S. (2020). Silk fibroin nanofibrous mats for visible sensing of oxidative stress in cutaneous wounds. *Biomaterials science*, 8(21), 5900–5910.
9. Jiang, W., Low, B. Q. L., Long, R., Low, J., Loh, H., Tang, K. Y., ... & Ye, E. (2023). Active site engineering on plasmonic nanostructures for efficient photocatalysis. *ACS nano*, 17(5), 4193–4229.
10. Wang, L., Zhu, W., Lu, W., Shi, L., Wang, R., Pang, R., ... & Xu, X. (2019). One-step electrodeposition of AuNi nanodendrite arrays as photoelectrochemical biosensors for glucose and hydrogen peroxide detection. *Biosensors and Bioelectronics*, 142, 111577.
11. Si, G., Zhao, Y., Lv, J., Lu, M., Wang, F., Liu, H., ... & Liu, Y. J. (2013). Reflective plasmonic color filters based on lithographically patterned silver nanorod arrays. *Nanoscale*, 5(14), 6243–6248.

12. Wang, L., Ng, R. J. H., Safari Dinachali, S., Jalali, M., Yu, Y., & Yang, J. K. (2016). Large area plasmonic color palettes with expanded gamut using colloidal self-assembly. *Acs Photonics*, 3(4), 627-633.
13. Innocenzi, P., Malfatti, L., & Soler-Illia, G. J. (2011). Hierarchical mesoporous films: from self-assembly to porosity with different length scales. *Chemistry of Materials*, 23(10), 2501-2509.
14. Zhang, J., Li, Y., Zhang, X., & Yang, B. (2010). Colloidal self-assembly meets nanofabrication: From two-dimensional colloidal crystals to nanostructure arrays. *Advanced materials*, 22(38), 4249-4269.
15. Choi, D. G., Jang, S. G., Kim, S., Lee, E., Han, C. S., & Yang, S. M. (2006). Multifaceted and nanobored particle arrays sculpted using colloidal lithography. *Advanced Functional Materials*, 16(1), 33-40.
16. del Real Mata, C., Yedire, S. G., Jalali, M., Siavash Moakhar, R., AbdElFatah, T., Kaur, J., ... & Mahshid, S. (2025). AI-Assisted Plasmonic Enhanced Colorimetric Fluidic Device for Hydrogen Peroxide Detection from Cancer Cells. *Advanced Materials Technologies*, 10(2), 2400633.
17. Doğan, V., Yüzer, E., Kılıç, V., & Şen, M. (2021). Non-enzymatic colorimetric detection of hydrogen peroxide using a µPAD coupled with a machine learning-based smartphone app. *Analyst*, 146(23), 7336-7344.
18. Xu, Q., Tang, Y., Zhu, P., Zhang, W., Zhang, Y., Solis, O. S., ... & Wang, J. (2022). Machine learning guided microwave-assisted quantum dot synthesis and an indication of residual H₂O₂ in human teeth. *Nanoscale*, 14(37), 13771-13778.
19. Kanuganti, S. R., Sultana, R., Kolli, D., Maddula, G. K., & Singampalli, M. R. (2023). Facile one pot synthesis of sulphur doped graphene for non-enzymatic sensing of hydrogen peroxide. *International Journal of Environmental Analytical Chemistry*, 103(19), 8051-8062. <https://doi.org/10.1080/03067319.2021.1980785>
20. del Real Mata, C., Jeanne, O., Jalali, M., Lu, Y., & Mahshid, S. (2023). Nanostructured-Based Optical Readouts Interfaced with Machine Learning for Identification of Extracellular Vesicles. *Advanced Healthcare Materials*, 12(5), 2202123.
21. Sergyan, S. (2008, January). Color histogram features based image classification in content-based image retrieval systems. In *2008 6th international symposium on applied machine intelligence and informatics* (pp. 221-224). IEEE.
22. Zebari, R. R., Majeed, M. G., Mohammed, M. Q., Abdhussain, Z. N., Kosimov, L., & Alchilibi, H. (2023, November). Dynamic Template Learning for Top-Level Computer Management Using Bayesian Optimization. In *2023 3rd International Conference on Advancement in Electronics & Communication Engineering (AECE)* (pp. 840-844). IEEE.
23. Qian, Y., Lin, J., Han, L., Lin, L., & Zhu, H. (2014). A resorufin-based colorimetric and fluorescent probe for live-cell monitoring of hydrazine. *Biosensors and Bioelectronics*, 58, 282-286.
24. Yan, J. W., Wang, X. L., Tan, Q. F., Yao, P. F., Tan, J. H., & Zhang, L. (2016). A colorimetric and fluorescent dual probe for palladium in aqueous medium and live cell imaging. *Analyst*, 141(8), 2376-2379.